

Articles

Environmental Mimic of Receptor Interaction: Conformational Analysis of CCK-15 in Solution

Stefania Albrizio,[†] Alfonso Carotenuto,[‡] Caterina Fattorusso,^{§,‡} Luis Moroder,^{||} Delia Picone,[⊥] Piero A. Temussi,[⊥] and Annamaria D'Ursi^{*,‡}

Dipartimento di Scienze Farmaceutiche, Università di Salerno, via Ponte Don Melillo 11 c, I-84084 Fisciano, Italy, Dipartimento di Chimica Farmaceutica e Tossicologica, Università di Napoli "Federico II", via Montesano 49, I-80131 Napoli, Italy, Dipartimento di Chimica, Università di Napoli "Federico II", via Cinthia, I-80126 Napoli, Italy, Dipartimento di Chimica delle Sostanze Naturali, Università di Napoli "Federico II", via Montesano 49, I-80131 Napoli, Italy, and Max Planck Institute für Biochimie, 82143, Martinsried, Germany

Received June 7, 2001

CCK-15, a peptide derived from the 115-membered CCK preprohormone, was the object of a comparative conformational analysis by NMR spectroscopy and molecular modeling methods. NMR data in several solvents demonstrate that the propensity of the peptide to fold into a helical conformation is intrinsic, not merely a consequence of the interaction with phosphatidylcholine micelles or with a putative receptor, as suggested by a previous study on CCK-8 (Pellegrini, M.; Mierke, D. *Biochemistry* **1999**, *38*, 14775–14783.). The prevailing CCK-15 conformer in a mixture 1,1,1,3,3,3-hexafluoroacetone/water reveals that the residues common to CCK-15 and CCK-8 assume very similar conformations. Our CCK-15 structure is consistent with the model of receptor interaction proposed by Pellegrini and Mierke and discloses possible novel interactions that involve a larger area of the putative receptor. The consensus structure between CCK-15 and CCK-8 shows a good superposition of the side chains of residues 12–14 with crucial moieties of two non-peptidic CCK-A antagonists.

Introduction

The peptide cholecystokinin CCK¹ is found throughout the gastrointestinal system and the central nervous system where it functions as both a hormone and a neurotransmitter. CCK was originally isolated from porcine intestine as a 33-membered peptide and has subsequently been shown to exist physiologically in multiple forms derived from the cleavage of a 115-membered preprohormone.^{2,3} The major physiological forms are CCK-58, CCK-39, CCK-33, and CCK-8, so designated by the number of residues counted backward from the commonly shared C-terminus.¹ Post-translational processing of CCK involves sulfation of tyrosine at position 7 from the C-terminus and amidation of the C-terminal phenylalanine residue¹ from the -Phe-Gly-OH biosynthetic precursors. Studies using chemically synthesized fragments have shown that the C-terminally sulfated and amidated heptapeptide is essential for full biological activity; however, fragments as small as the C-terminal pentapeptide, which CCK has in common with the related peptide gastrin, and the C-terminal tetrapeptide retain biological activity.⁴ The

actions of CCK are mediated by specific high-affinity membrane receptors on target cells. These receptors have been pharmacologically and biologically characterized and are divided into two subtypes based on their affinities for CCK and gastrin.^{5–7} The CCK-A subtype has an approximately 500-fold higher affinity for CCK than for gastrin, while the CCK-B/G subtype has the same high affinity for both CCK and gastrin. The cloning of the cDNA for these receptors has shown them to belong to the superfamily of G-protein-coupled receptors that are characterized by seven transmembrane domains connected by intracellular and extracellular loops with an extracellular N-terminal and intracellular C-terminal extension.⁸

A recent conformational study⁹ has shown that the extracellular N-terminal domain of the CCK-A receptor subtype assumes a regular, ordered conformation in an aqueous solution of phosphatidylcholine micelles. Moreover, unsulfated CCK-8 was shown to bind to this receptor fragment with the formation of a well-defined helical structure.

It is important to understand whether the anisotropic nature of the micellar solution plays a crucial role in determining the conformation of the CCK agonist that binds to the receptor. Accordingly, we undertook a detailed conformational analysis of CCK-15 in isotropic media, particularly in helix-inducing solvents. The choice of CCK-15, instead of CCK-8, which coincides with its C-terminal part, has the further advantage of unveiling new potential receptor interaction points.

* To whom correspondence should be addressed. Phone: +39 089 964355. Fax: +39 089 962828. E-mail: dursi@unisa.it.

[†] Dipartimento di Chimica Farmaceutica e Tossicologica, Università di Napoli "Federico II".

[‡] Università di Salerno.

[§] Dipartimento di Chimica delle Sostanze Naturali, Università di Napoli "Federico II".

^{||} Max Planck Institute für Biochimie.

[⊥] Dipartimento di Chimica, Università di Napoli "Federico II".

Here, we present a solution study of CCK-15 in water, DMSO, DMSO/water, and 1,1,1,3,3,3-hexafluoroacetone/water (HFA/water) by CD and NMR spectroscopies. The solution structure, determined by NMR, is compared with the conformation of unsulfated CCK-8 docked onto the N-terminal domain of the CCK-A receptor subtype.

Results and Discussion

Circular Dichroic Properties of CCK-15. A preliminary screening of the conformational preferences of CCK-15 as a function of the environment was performed by means of CD spectroscopy. As reported previously,¹⁰ the spectrum in water lacks any of the features typical of canonical secondary structures, suggesting that CCK-15, like most short linear peptides, assumes a disordered conformation in water. While in surfactants CCK peptides of increasing chain length¹⁰ as well as the lipo-derivatized CCK-9¹¹ were found to exhibit CD spectra typical of β -sheet type structures, in lipid bilayers the lipo-derivatized CCK-9 assumes a helical conformation.¹² Similarly, the CD spectra of CCK-15 recorded in HFA/water (50:50, v/v) shows the double-well shape typical of helical structures. Consistent with its exceptional helix-inducing properties, the HFA/water mixture favors the highest α -helix content of CCK-15, but it is worth noting that, according to NMR data (vide infra), CCK-15 is helical even in DMSO/water, a result consistent with older findings on CCK-9.¹³ Since mixtures of DMSO/water generally favor extended structures or isolated turns, detection of substantial helical content in this solvent indicates that CCK-15 has a strong intrinsic tendency to assume a helical conformation.

NMR Conformational Analysis. The conformational preferences of CCK-15 were investigated in greater depth by means of NMR spectroscopy. Exploratory NMR spectra were run in water, DMSO, DMSO/water (80:20, v/v), TFE/water (70:30, v/v), and HFA/water (50:50, v/v) solutions. Since CD spectra in water are consistent with a completely disordered structure, we limited the quantitative NMR study of CCK-15 to the solution in HFA/water that can probe the tendency of the CCK-15 peptide to assume helical conformations and to DMSO/water to test the possibility of structuring CCK-15 in media with physicochemical features consistent with transport fluids, i.e., extracellular aqueous solution. Alcohols, either neat or mixed with water, are the most popular media used to induce helicity in peptides.^{14–16} In addition to the common alcohols quoted in these references, HFA/water mixtures have been proposed. These behave like TFE/water mixtures but with a much higher helix-inducing propensity.¹⁷ Such a propensity, however, does not override the intrinsic tendency linked to the sequence of specific residues. We have shown in a paradigmatic case, i.e., that of β -endorphin,¹⁸ that even in a strong helix-inducing solvent there can be coexistence of helical and disordered stretches, depending on the intrinsic tendency of the residues. As a medium compatible with transport fluids, we employed a DMSO/water mixture, a medium that has a viscosity close to that of the intersynaptic fluid. Typical viscosities of cytoplasm range from 5 to 30 cP,¹⁹ and it has been postulated²⁰ that they play an important role in cell communication processes. Viscosities on the

order of those of cytoplasm are easily reproduced by cryoprotective mixtures.^{21–23} In addition, the use of a viscous solvent medium can affect the equilibrium among isoenergetic conformers, selecting the more ordered conformers.²⁴

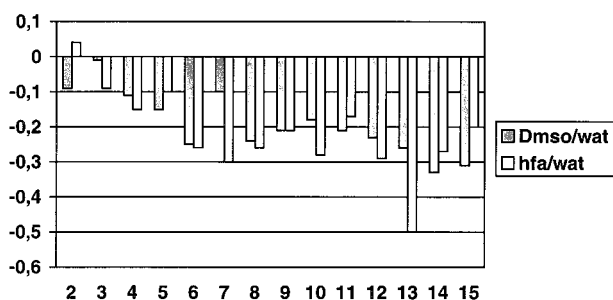
Whole sets of 1D and 2D ¹H homonuclear NMR spectra in DMSO/water (80:20, v/v) and HFA/water (50:50, v/v) were acquired on a Bruker DRX 600 at 300 K. To find optimal conditions of concentration and to avoid problems from aggregation phenomena, 1D ¹H NMR spectra in HFA/water mixtures were recorded in the concentration range 0.5–15 mM. Complete assignments of the proton spectra of CCK-15 were obtained by standard procedures²⁵ DQF-COSY,²⁶ TOCSY,²⁷ and NOESY²⁸ experiments were used for spin system identification. Sequence-specific backbone NMR signal assignments were done by means of NOESY²⁸ experiments with the aid of XEASY software package.²⁹

Table 1 reports the complete proton chemical shift assignment of backbone protons of CCK-15 in DMSO/water and in HFA/water. CH_α chemical shifts can also be used to analyze the secondary structure content, particularly via the so-called chemical shift index.^{30,31} An increase of helicity induces an upfield shift of CH_α resonances corresponding to a negative variation of the chemical shifts ($\Delta\delta H_{\alpha}$) relative to a random coil conformation. In Figure 1 the differences between the CH_α chemical shifts measured in HFA/water and in DMSO/water, and those reported for the corresponding residues in random coil, are plotted for each residue of the CCK-15. The departures from typical random coil values are comparable for the two different mixtures. CH_α protons experience remarkable upfield shifts in both media, suggesting the presence of turns and/or helical conformation.²⁵ A sizable difference is detectable only for Met-13 where the CCK-15 in HFA/water appears significantly more ordered. The ³J_{NH-αCH} coupling constants, measured by means of the procedure of Titman and Keeler³² based on a processing of DQF-COSY²⁶ and TOCSY spectra,²⁷ point in the same direction. Small values of these coupling constants are typical of turns or helical conformations, whereas ³J_{NH-αCH} coupling constants higher than 6 Hz reflect random or extended conformations.³² Most of the measured values of the ³J_{NH-αCH} coupling constants are in fact smaller than 5 Hz, particularly for residues located in the C-terminal region, whereas larger values of the coupling constants are observed for the N-terminal residues.

The amide and the fingerprint regions of the NOESY spectra (300 K, 600 MHz, tm 300 ms) of CCK-15 recorded in DMSO/water and in HFA/water are reported in Figure 2. The high number of well-resolved cross-peaks is consistent with the prevalence of ordered conformers in both solvent mixtures. It is also clear, however, that only the data in HFA/water are of sufficiently high quality to warrant a detailed structure calculation. Several sequential cross-peaks relevant for the assignment and for the structure calculation are labeled in the Figure 2. A qualitative analysis of NOE sequential and medium-range connectivities of CCK-15 in HFA/water shows that terminal residues are disordered, but the whole sequence is characterized by a series of sequential NH_{*i*}-NH_{*i*+1} NOEs, consistent with a nascent helical structure,³³ and diagnostically critical

Table 1. Relevant Proton Chemical Shifts (ppm) of CCK-15 in DMSO/Water 80:20 v/v and HFA/Water 50:50 v/v at 600 MHz and 300 K

residue	solvent	NH	CH _α	H _{β2}	H _{γ2}	H _δ	H _ε	others
HIS2	water/DMSO		4.55	3.073/2.95		6.91	7.69	
	water/HFA	8.59	4.68	3.07/3.07		7.13	8.36	
ARG3	water/DMSO	8.37	4.37	1.65/1.51	1.79	3.12		
	water/HFA	8.21	4.29	1.53	1.75/1.67	3.05	6.95	
ILE4	water/DMSO	8.45	4.12	1.85	1.45			
	water/HFA	7.85	4.08	1.781	1.37/1.09 CH3 _γ 0.82	0.77		
SER5	water/DMSO	7.96	4.36	3.76/3.65				
	water/HFA	7.81	4.40	3.73/3.93				
ASP6	water/DMSO	8.23	4.51	2.65/2.54				
	water/HFA	8.12	4.50	2.74				
ARG7	water/DMSO	7.96	4.28	1.56/1.48	1.68			
	water/HFA	7.90	4.08	1.50	1.65	3.01	6.82	
ASP8	water/DMSO	8.17	4.52	2.61/2.53				
	water/HFA	7.84	4.50	2.59/2.67				
TYR9	water/DMSO	8.17	4.39	2.95/2.80		7.20	7.10	
	water/HFA	7.69	4.39	2.94/3.08		7.13	6.69	
MET10	water/DMSO	8.22	4.34	2.35/2.23	2.94/2.39			
	water/HFA	7.81	4.24	2.35/2.44	1.79/1.87			
GLY11	water/DMSO	8.28	3.76					
	water/HFA	7.76	3.82/3.77					
TRP12	water/DMSO	8.36	4.47	3.21/3.12				Hz2 7.39; Hz3 6.99; HH2 7.11
	water/HFA	7.44	4.41	3.16/3.29		7.14	9.53	Hz2 7.36
MET13	water/DMSO	8.42	4.26	1.90/1.84	2.41/2.33			
	water/HFA	7.47	4.00	1.60/1.90				
ASP14	water/DMSO	7.96	4.44	2.51/5.21				
	water/HFA	7.67	4.48	2.53/2.64				
PHE15	water/DMSO	7.91	4.35	3.15/2.90		7.00	7.40	
	water/HFA	7.60	4.46	2.95/3.11	7.15	6.70		

**Figure 1.** Chemical shift differences with respect to typical random coil values for CH_α protons of CCK-15 in HFA/water and in DMSO/water vs residue number.

(*i, i + 2*) and (*i, i + 3*) effects typical of a regular α -helix can be observed for the whole 7–14 stretch.

Structure Calculation. Detailed three-dimensional structures were calculated by simulated annealing in torsion angle space and restrained molecular mechanics based on 147 NOE-derived restraints, using DYANA software package.³⁴ The best 10 calculated structures were considered for further calculations. The structures were energy-minimized using the Discover module of the Insight 2000 software (MSI, San Diego). Unrestrained energy minimizations were performed using a dielectric constant value $\epsilon = 1$. Despite the strict convergence criterion used (0.001) and the lack of solvent molecules, the NMR calculated structures showed a high degree of stability when relaxed without constraints (rmsd = 0.9 Å). Figure 3a shows the overlap of the 10 best structures of CCK-15 after unrestrained

minimization of those generated by DYANA calculations. The fit was calculated on residues 4–13, i.e., excluding terminal residues, and yielded good rmsd values both for backbone atoms (0.46 Å) and all heavy atoms (1.08 Å). The quality of the NMR structural determination can also be inferred from the limited spread of the corresponding side chains (Figure 3b). All residues of the segment 4–13 have canonical conformations, but only the stretch 7–12 assumes a regular helical conformation.

As mentioned in the Introduction, the structure of non-sulfated CCK-8 has been recently characterized in DPC micelles as part of the complex with the N-terminus of the CCK-A receptor (CCK-A 1–47).⁹ It is interesting to compare our structure of CCK-15, determined in an isotropic medium, with the corresponding segment of CCK-8, recorded in the previously mentioned micellar environment. Figure 4a shows the superposition of α -carbons of residues 8–13 of the CCK-15 conformer of lowest energy, with the corresponding atoms of CCK-8 (PDB code, 1d6g). The good fit between the two structures (rmsd = 0.818 Å) indicates that the CCK-15 solution structure and the CCK-8 structure complexed with the putative receptor have very similar backbone secondary structure. The CCK-15 conformer of lowest energy was selected to perform subsequent calculations. Since the structure of non-sulfated CCK-8 used in the comparison is part of a complex, it is not obvious whether the CCK-A receptor plays a relevant role in limiting the peptide accessible conformational space. To find out whether the receptor can affect the

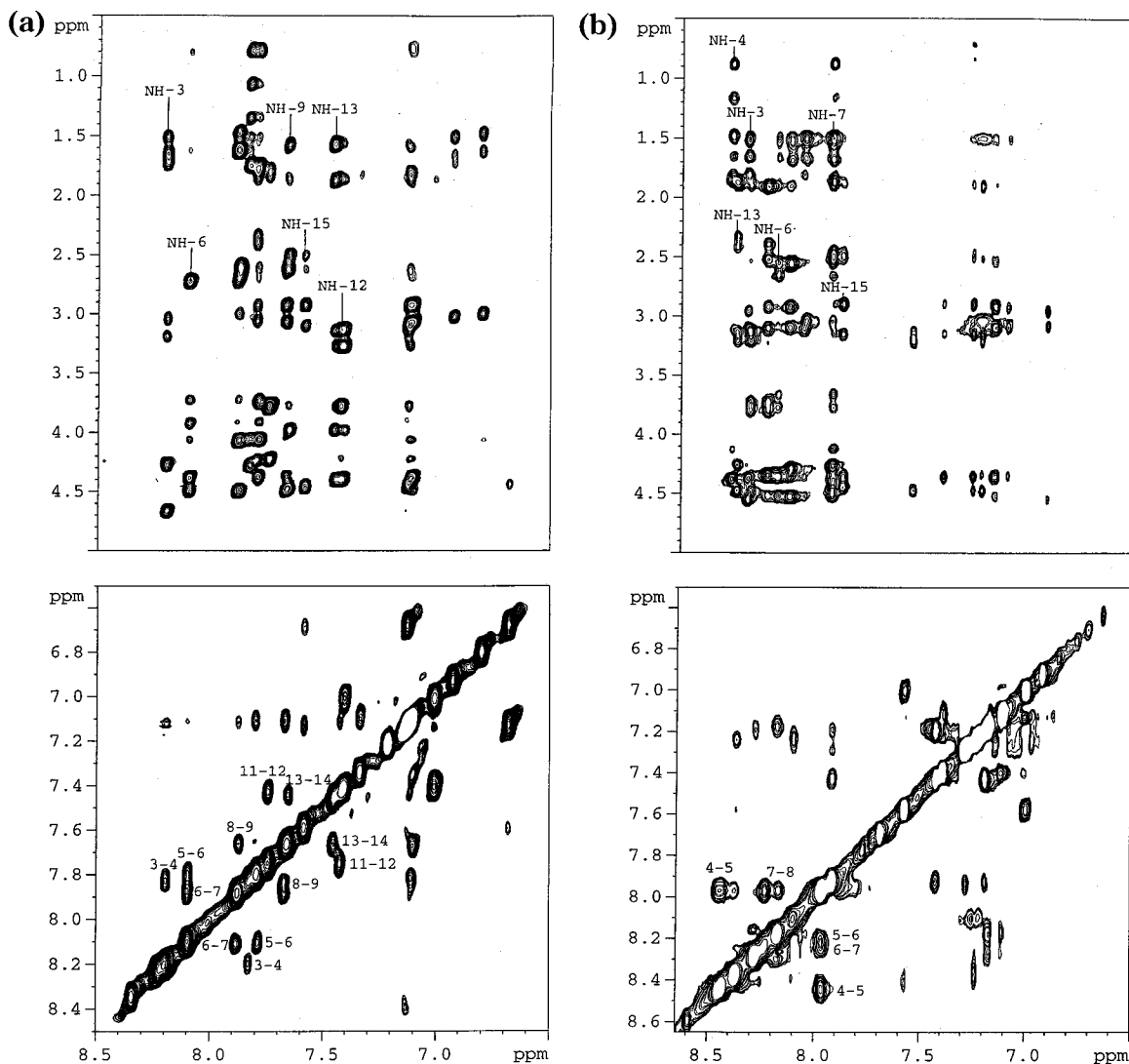


Figure 2. Amide and the fingerprint regions of the NOESY spectra (300 K, 600 MHz, t_m 300 ms) of CCK-15 collected in DMSO/water (a) and in HFA/water (b).

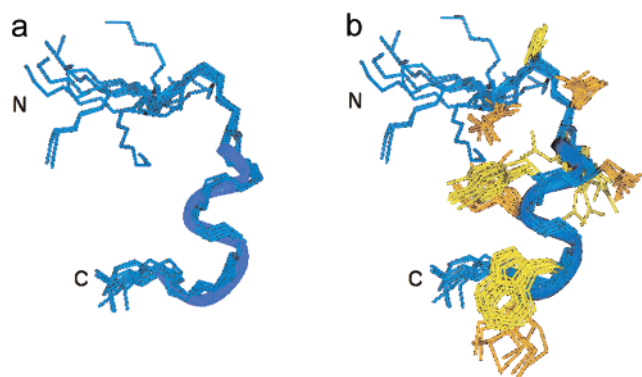


Figure 3. Superposition of the 10 best structures of the CCK-15 peptide obtained from DYANA structure calculations and following minimization using the Discover module of the Insight 2000 software. The fit was based on the backbone heavy atoms (N, C $^{\alpha}$, C) of residues Ile4–Met13. (a) Only the backbone structures are displayed. (b) Peptide backbones with side chains of residues Ile4–Met13 are shown.

conformation of CCK-15, we performed a docking of our structure on the receptor fragment by means of molecular mechanics and dynamics calculations using as a starting model for the receptor the 1–47 region of

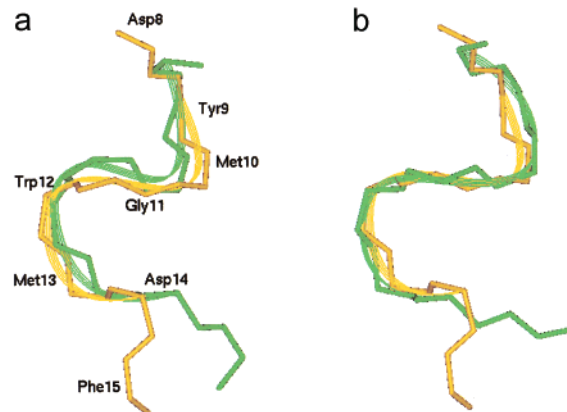


Figure 4. Superposition of α -carbons of residues Asp8–Met13 of the lowest energy CCK-15 conformer with the corresponding atoms of CCK-8 (PDB code, 1d6g). For CCK-15 the structure obtained before (a) and after (b) docking with the 1–47 region of the CCK-A receptor model, reported by Pellegrini and Mierke,⁹ was considered.

CCK-A reported by Pellegrini and Mierke.⁹ Figure 4b shows the superposition of α -carbons of residues 8–13 of the CCK-15 with the corresponding atoms of CCK-8 after further refinement of the CCK-15 conformer in the

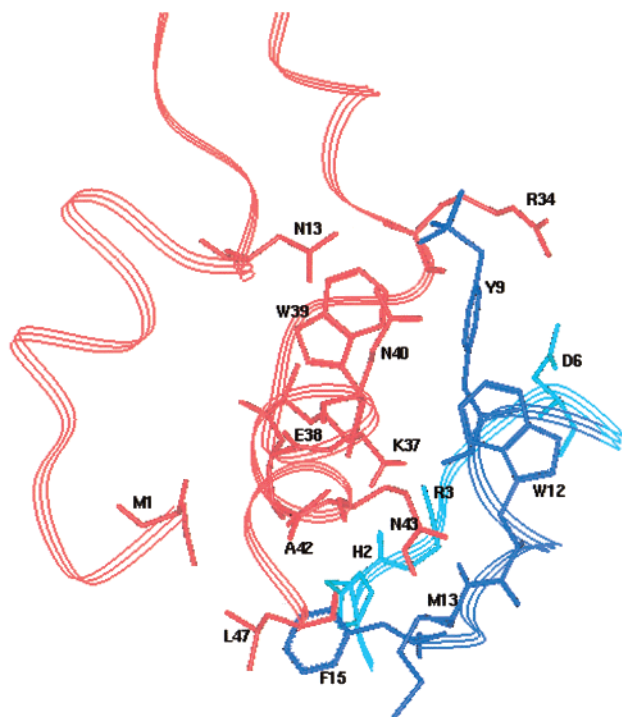


Figure 5. Schematic representation of the complex between the 1–47 region of the CCK-A receptor (red ribbon) and that of the CCK-15 (blue ribbon). The dark-blue ribbon represent residues common to CCK-15 and CCK-8 (8–15), and the light-blue ribbon represents residues belonging to CCK-15 only (1–7). The side chains of the CCK-15 residues and of CCK-A receptor involved in the main interactions are shown with the corresponding colors and labeled.

presence of the CCK-A receptor fragment 1–47, i.e., after a global refinement following docking. The rmsd value relative to the 8–13 α -carbons, after this “docking refinement”, decreases from 0.818 Å to a value of 0.650 Å. Figure 4b shows that superposition of residues 8–13 is clearly improved, whereas residues 14 and 15 are still diverging from the corresponding residues in CCK-8 but with a different orientation.

The conformational features of the residues involved in the interaction with the receptor were further analyzed. Figure 5 shows the models of the CCK-A receptor, represented as a red ribbon, and of the CCK-15 agonist, represented as a blue ribbon. Two shades of blue were used for residues common to CCK-8 (8–15, dark hue) and for those of CCK-15 only (1–7, light hue). The side chains of the CCK-15 residues involved in the main interactions are shown with corresponding colors and labeled, whereas those of the CCK-A receptor are shown without labels to avoid confusion. The side chains of Tyr9, Trp12, and Met13 that cover a sizable portion of the interaction surface of the peptides with the model CCK-A receptor show differences with respect to the structure of isolated CCK-15 in solution as a result of the molecular refinement of the CCK-15 conformation in the presence of the CCK-A receptor. In the complex CCK-15/receptor all the relevant intermolecular interactions occurring in the CCK-8 structure of Pellegrini and Mierke⁹ can still be observed. The most prominent among these are two hydrogen bonds, both involving the side chain of CCK-A Gln43 and backbone atoms of Met13, i.e., one between the side chain NH of Gln43 and

the backbone carbonyl oxygen of CCK-15 Met13 and another between the CCK-A Gln43 side chain carbonyl oxygen and CCK-15 Met13 amide backbone proton. Furthermore, there is a close contact between the aromatic rings of CCK-A Trp39 and CCK-15 Tyr9 that are approximately perpendicular. This interaction is a typical aromatic–aromatic interaction that is known to stabilize peptide and protein tertiary structures. The edge-to-face orientation is caused by the electrostatic attraction between the positively charged protons (Tyr9) and the negatively charged carbon atoms on the aromatic ring (Trp39).

In addition, new contact sites involving residues not present in CCK-8 can now be observed. The new contacts extend the area of interaction of CCK-15 on the same side of the receptor involved in the complex with CCK-8, as shown in Figure 5. The two main residues characterizing the new contacts are His2 and Arg3. The ammonium group of the CCK-A Lys37 side chain is placed between the carbonyl oxygens of His2 and Arg3 at distances consistent with the formation of two hydrogen bonds. The imidazole ring of His2 is involved in a likely electrostatic interaction with the carbonyl of the CCK-A Glu38 side chain. There are new relevant interactions involving Phe15, which is common to CCK-8 and CCK-15 but whose side chain had a different orientation in the quoted work.⁹ The CCK-15 Phe15 side chain interacts with three aliphatic CCK-A residues, namely, Met1, Ala42, and Leu47, thus tightening considerably the interactions of this hydrophobic core. These novel observations are fully consistent with the study of photoaffinity cross-linking by Ding et al.,³⁵ which emphasizes the importance of the N-terminal domain of the receptor and which apparently protects the peptide-binding domain within the receptor. The model of Figure 5 shows that, owing to these additional interactions, CCK-15 covers a larger area of the putative receptor surface. It is also interesting to note that the sulfate group of Tyr9, which is responsible for the full bioactivity of the CCK peptides and is present in the analyzed CCK-15 model, is close to CCK-A Trp39 and Gln40, in full agreement with previously reported experimental mutagenesis data that pointed to a critical role of these two residues.³⁶ The sulfate group of Tyr9 is also proximal to the CCK-A Arg34, a positively charged amino acid, while the amide proton of the CCK-A Asn13 side chain is placed at 2.8 Å from a sulfate oxygen, consistent with the formation of a hydrogen bond. These interactions may account for the importance of the post-translational sulfation in terms of receptor subtype specificity. All these data yield strong evidence for a high degree of similarity between the receptor-bound CCK-8 and CCK-15, in full agreement with their identical receptor affinities.¹⁰ The data also validate the consensus structure as a possible bioactive conformation that can be used for further drug design.

Structural comparison of this putative bioactive structure with those of well-established CCK-A receptor antagonists would suggest similarities in the spatial array, particularly of the aromatic moieties. It is crucial, for such a comparison, to assume that peptides and non-peptidic ligands interact with the same active site of the receptor. Recent mutagenesis data apparently suggest a distinct binding mode for the peptidic agonists

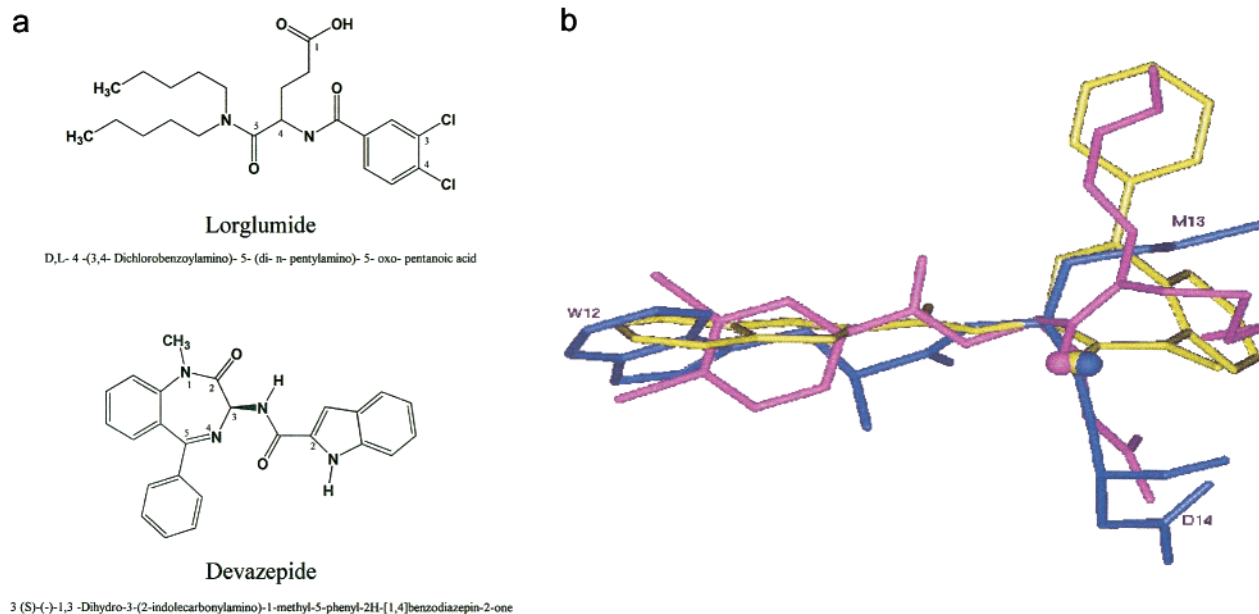


Figure 6. (a) Chemical structures of the non-peptidic CCK-A receptor ligands lorglumide and devazepide. (b) Superposition of the NMR-derived structure of the CCK-15 peptide with the X-ray diffraction structures of the non-peptidic CCK-A receptor ligands devazepide and lorglumide.

and non-peptide antagonists.^{37–43} Peptide/benzodiazepine hybrids were recently used to study in detail this open question, and the results would support a different binding mode with the peptides interacting mainly with the extracellular surface of the receptor and antagonists inserted into a deeper hydrophobic pocket.⁴⁴ Nonetheless, it seems fair to hypothesize that peptides can interact with both sites, and accordingly, it remains of interest to compare the two classes of compounds.

Since CCK is involved in many different biological processes such as gut function, digestive processes, control of feeding behavior, and neurotransmitter release, the therapeutic potential of cholecystokinin receptors ligands seems extremely broad and promising. Several families of CCK receptor ligands (peptides, peptidomimetics, peptoids, or non-peptidic compounds) were prepared with the aim of improving agonistic or antagonistic potency and selectivity. Non-peptide CCK-A (gastrin) antagonists were developed as potential therapeutic agents. The reference CCK antagonist compound was, for several years, proglumide, but chemical modifications of its structure led to a new series of CCK receptor antagonists whose most representative compound is lorglumide.⁴⁵ The isolation and identification of asperlicin as a selective CCK antagonist⁴⁶ led to the subsequent development of selective and potent CCK benzodiazepine derivatives, devazepide being the most active and selective as a CCK-A antagonist.⁴⁷ In Figure 6 the backbone of residues 12–14 of the calculated CCK-15 model is overlapped to the crystal structures (Cambridge Crystallographic Database) of representative non-peptide CCK-A receptor ligands, such as lorglumide and devazepide. The fitting was performed using the centromers of corresponding rings and/or side chains of lorglumide, devazepide, and residues 12–14 of CCK-15.

As expected, the fit of the rings or groups directly involved in the fitting procedure is good (Figure 6b). However, it is very interesting to note that an optimal

superposition is also detectable for the carbonyl oxygens of the Met13 backbone, the devazepide benzodiazepinonic ring, and the lorglumide 5-oxo function, which were not used at all in the fitting (Figure 6b). It is also worth noting that the indolyl moieties of Trp12 and devazepide do not simply occupy the same region in space, as imposed by the fitting procedure, but they actually have the same orientation as the lorglumide 3,4-dichlorophenyl ring. It is interesting that devazepide and lorglumide have an orientation that allows H-bond interactions with CCK-A Gln43. These results are in agreement with structure–activity relationships of CCK-A antagonists.

Conclusion

The study of the solution conformation of CCK-15 in several solvents by NMR and modeling techniques was undertaken with two main goals: to ascertain whether the helical conformation found for CCK-8 in micellar solution was mainly induced by the environment and to find further interaction points with the receptor. The prevailing structure in a mixture hexafluoroacetone/water, an isotropic medium, showed that the residues common to CCK-15 and CCK-8 have very similar conformations. The similarity is enhanced by concerted modeling together with the partial receptor structure proposed by Pellegrini and Mierke (1999) and discloses novel interactions that involve a large receptor area. Last but not least, the consensus structure between CCK-15 and CCK-8 is fully consistent with the architecture of two non-peptidic CCK-A antagonists.

Experimental Procedures

Peptide Synthesis. The CCK-15 peptide was synthesized as reported previously.⁴⁸

Circular Dichroism Spectroscopy. Circular dichroism (CD) spectra were obtained on a Jasco 810 spectropolarimeter at room temperature. Spectra were recorded with a path length of 0.1 cm, a bandwidth of 0.1 nm, a time constant of 2.0 s, and

a wavelength range of 190–260 nm, using quartz cuvettes. The CCK15 concentration was 100 μ M, and the pH was 7. The concentration was determined accurately by UV spectroscopy using ϵ_{280} for tryptofan.

The spectrum of the buffer was subtracted from all the other spectra; the results of 10 scans were then averaged.

NMR Spectroscopy. The sample for NMR spectroscopy was prepared by dissolving the appropriate amount of CCK-15 in 0.5 mL of $^1\text{H}_2\text{O}$ phosphate buffer (pH 6.6) to obtain a 1 mM solution. Lyophilized peptide was dissolved in 8 mM sodium phosphate buffer containing 50% 1,1,1,3,3,3-hexafluoroacetone trihydrate.

NMR spectra were recorded on a Bruker DRX-600 spectrometer. One-dimensional (1D) NMR spectra were recorded in the Fourier mode with quadrature detection, and the water signal was suppressed by low-power selective irradiation in the homogated mode. DQF-COSY,²⁶ TOCSY,²⁷ and NOESY²⁸ experiments were run in the phase-sensitive mode using quadrature detection in 1 by time-proportional phase increase of the initial pulse.⁴⁹ Data block sizes were 2048 addresses in t_2 and 512 equidistant t_1 values. Before Fourier transformation, the time domain data matrices were multiplied by shifted \sin^2 functions in both dimensions. A mixing time of 70 ms was used for the TOCSY experiments. NOESY experiments were run at 300 K with mixing times in the range 150–300 ms. The qualitative and quantitative analyses of DQF-COSY, TOCSY, and NOESY spectra were obtained using the interactive program package XEASY.²⁹ The NOE-based distance restraints were obtained from NOESY spectra collected with a mixing time of 250 ms. The NOE cross-peaks were integrated with the XEASY program (ETH), and they were converted into upper distance bounds using the CALIBA module of DYANA software.³⁴ Cross-peaks that overlapped more than 50% were treated as weak restraints in the DYANA calculation. An ensemble of 50 structures was generated with a distance geometry simulated annealing program DYANA using 147 NOE-based distance constraints. No dihedral angle restraints and no hydrogen bond restraints were used.

Molecular Modeling. A total of 50 NMR constrained structures were calculated by DYANA (standard protocol). The first 10 best scored ones showed an rmsd value of 0.4 Å, thus revealing a very high degree of similarity between each other. Therefore, this family was considered for further calculations. All energetic calculations were carried out using the Discover module present in the MSI InsightII software, using the $4r$ force field and applying a dielectric constant value of $4r$ to simulate the protein–protein interaction environment.

To check how much the imposed constraints influence the obtained structure, first it was relaxed without constraint by using a combination of steepest descent and conjugate gradient minimization algorithms until the maximum rms derivative was less than 0.01 kcal/Å. The resulting structure showed an rmsd value of 0.9 on C atoms from the original one.

The structure was then superimposed onto the one derived from the protein data bank (PDB code 1D6G)⁹ in which the CCK-8 peptide is complexed with a 47-amino acid, N-terminal fragment of the CCK-A receptor binding site. The superimposition was made using the C atoms of residue 8–13 of CCK-15 corresponding to residues 1–6 of CCK-8 not taking into account the last two carboxy-terminal amino acids that do not present a defined structured conformation in our calculations. The obtained rmsd value was 0.818 Å. CCK-8 present in the CCK-A binding site was thus replaced by CCK-15, and the complex was energetically minimized using the conjugate gradients method until the maximum rms derivative was less than 0.01 kcal/Å and applying a dielectric constant value of $4r$. The following restraints were applied during the calculations: CCK-A backbone fixed and CCK-15 backbone tethered with a template force constant of 10 kcal/Å². Distance constraints were imposed on CCK-8 Met13 NH and oxygen backbone atoms so that they have to be within a range of 1.6–2.5 Å from CCK-A Asn43 oxygen and from NH side chain atoms. A generic distance maximum force constant of 100 kcal/

mol and upper and lower distance force constants of 10 kcal/mol were used.

The complex geometrically optimized was then subjected to 60 ps of molecular dynamics calculations after an equilibration period of 30 ps using a temperature of 310 K, applying the same restraints mentioned above. During molecular dynamics, frame structures were saved every 1 ps. The average conformation was extracted and again energetically minimized without using any constraints by a combination of steepest descent and conjugate gradients minimization algorithms until the maximum rms derivative was less than 0.01 kcal/Å. The resulting CCK-15 conformation was again superimposed on CCK-8, using the same criterion previously described, with an rmsd value of 0.650 Å.

Complex bond distances, bond angles, and torsion angles were checked for their consistency with proteins standard values using the Homology InsightII module.

CCK-A residues displaying interactions with CCK-15 were checked for their conservation between CCK-A and CCK-B human, mouse, and rat receptors. Corresponding sequences were aligned using the PAM 120 matrix and the multiple alignment algorithm present in the Homology InsightII module.

Lorglumide and devazepide structures were extracted from the Cambridge Crystallographic Data Bank and fitted upon CCK-15 conformation complexed with the CCK-A binding site.

References

- Rehfeld, J. F.; Van Soulinge, W. W. The tumor biology of gastrin and cholecystokinin. *Adv. Cancer Res.* **1994**, *63*, 295–347.
- Mutt, V.; Jorpes, J. E. Isolation of aspartyl-phenylalanine amide from cholecystokinin. *Biochem. Biophys. Res. Commun.* **1967**, *26*, 392–397.
- Deschenes, R. J.; Lorenz, L. J.; Haun, R. S.; Roos, B. A.; Collier, K. J.; Dixon, J. E. Cloning and sequence analysis of a cDNA encoding rat preprocholecystokinin. *Proc. Natl. Acad. Sci. U.S.A.* **1984**, *81*, 726–730.
- Jensen, R. T.; Lemp, G. F.; Gardner, J. D. Interactions of COOH-terminal fragments of cholecystokinin with receptors on dispersed acini from guinea pig pancreas. *J. Biol. Chem.* **1982**, *257*, 5554–5559.
- Wank, S. A. Cholecystokinin receptors. *Am. J. Physiol.* **1995**, *32*, 628–646.
- Ulrich, C. D.; Ferber, I.; Holicky, E.; Hadac, E.; Buell, G.; Miller, L. J. Molecular cloning and functional expression of the human gallbladder cholecystokinin A receptor. *Biochem. Biophys. Res. Commun.* **1993**, *193*, 204–211.
- Silvente-Poirot, S.; Dufresne, M.; Vaysse, N.; Fourmy, D. The peripheral cholecystokinin receptors. *Eur. J. Biochem.* **1993**, *215*, 513–529.
- Deweert, A.; Pisegna, J. R.; Huppi, K.; Wank, S. A. Molecular cloning, functional expression and chromosomal localization of the human cholecystokinin type A receptor. *Biochem. Biophys. Res. Commun.* **1993**, *194*, 811–818.
- Pellegrini, M.; Mierke, D. Molecular complex of cholecystokinin-8 and N-terminus of the cholecystokinin A receptor by NMR spectroscopy. *Biochemistry* **1999**, *38*, 14775–14783.
- Moroder, L.; Romano, R.; Weyher, E.; Svoboda, M.; Christophe, J. Circular dichroism study of fully bioactive CCK-peptides of increasing chain length. *Z. Naturforsch.* **1993**, *48b*, 1419–1430.
- Romano, R.; Bayerl, T. M.; Moroder, L. Lipophilic derivatization and its effects on the interaction of cholecystokinin (CCK) nonapeptide with phospholipids. *Biochim. Biophys. Acta.* **1993**, *1151*, 111–119.
- Moroder, L.; Romano, R.; Guba, W.; Mierke, D. F.; Kessler, H.; Delporte, C.; Winand, J.; Christophe, J. New evidence for a membrane-bound pathway in hormone receptor binding. *Biochemistry* **1993**, *32*, 13551–13559.
- Moroder, L.; D'Ursi, A.; Picone, D.; Amodeo, P.; Temussi, P. A. Solution conformation of CCK9, a cholecystokinin analog. *Biochem. Biophys. Res. Commun.* **1992**, *190*, 741–746.
- Hamada, D.; Kuroda, Y.; Tanaka, T.; Goto, Y. High helical propensity of the peptide fragments derived from beta-lactoglobulin, a predominantly beta-sheet protein. *J. Mol. Biol.* **1995**, *254*, 737–746.
- Shiraki, K.; Nishikawa, K.; Goto, Y. Trifluoroethanol-induced stabilization of the alpha-helical structure of beta-lactoglobulin: implication for non-hierarchical protein folding. *J. Mol. Biol.* **1995**, *254*, 180–194.
- Sonnichsen, F. D.; Van Eyk, J. E.; Hodges, R. S.; Sykes, B. D. Effect of trifluoroethanol on protein secondary structure: an NMR and CD study using a synthetic actin peptide. *Biochemistry* **1992**, *31*, 8790–8798.

- (17) Rajan, R.; Awasthi, S. K.; Bhattachajya, S.; Balaran, P. Teflon-coated peptides: hexafluoroacetone trihydrate as a structure stabilizer for peptides. *Biopolymers* **1997**, *42*, 125–128.
- (18) Saviano, G.; Crescenzi, O.; Picone, D.; Temussi, P. A.; Tancredi, T. Solution structure of human β -endorphin in helicogenic solvents: A NMR study. *J. Pept. Sci.* **1999**, *5*, 410–422.
- (19) Pollard, E. C. In *The Aqueous Cytoplasm*; Keith, A. D., Ed.; Marcel Dekker: New York, 1976; pp 1–22.
- (20) Chapmann, D.; Peel, W. E. In *The Aqueous Cytoplasm*; Keith, A. D., Ed.; Dekker: New York, 1976; pp 175–196.
- (21) Douzou, P.; Petsko, G. A. Proteins at work: "stop-action" pictures at subzero temperatures. *Adv. Protein Chem.* **1984**, *36*, 245–361.
- (22) Fink, A. L. Protein folding in cryosolvents at subzero temperatures. *Methods Enzymol.* **1986**, *131*, 173–187.
- (23) Tobias, B.; Markley, J. L. Carbon-13 NMR relaxation of [1–13C] acetyl-chymotripsin dissolved in a cryosolvent at subzero temperatures. *J. Magn. Reson.* **1986**, *68*, 381–385.
- (24) Amodeo, P.; Motta, A.; Picone, D.; Saviano, G.; Tancredi, T.; Temussi, P. A. Viscosity as a conformational sieve. NOE of linear peptides in cryoprotective mixtures. *J. Magn. Reson.* **1991**, *95*, 201–207.
- (25) Wüthrich, K. In *NMR of Proteins and Nucleic Acids*; Wiley: New York, 1986; pp 162–175.
- (26) Piantini, U.; Soerensen, O. W.; Ernst, R. R. Multiple quantum filters for elucidating NMR coupling networks. *J. Am. Chem. Soc.* **1982**, *104*, 6800–6801.
- (27) Bax, A.; Davis, D. G. Mlev-17-based two-dimensional homonuclear magnetization transfer spectroscopy. *J. Magn. Reson.* **1985**, *65*, 355–360.
- (28) Jeener, J.; Meyer, B. H.; Bachman, P.; Ernst, R. R. Investigation of exchange processes by two-dimensional NMR spectroscopy. *J. Chem. Phys.* **1979**, *71*, 4546–4553.
- (29) Bartels, C.; Xia, T.; Billeter, M.; Guentert, P.; Wüthrich, K. The program XEASY for computer-supported NMR spectral analysis of biological macromolecules. *J. Biomol. NMR* **1995**, *6*, 1–10.
- (30) Wishart, D. S.; Sykes, B. D.; Richards, F. M. Relationship between nuclear magnetic resonance chemical shift and protein secondary structure. *J. Mol. Biol.* **1991**, *222*, 311–333.
- (31) Wishart, D. S.; Sykes, B. D.; Richards, F. M. The Chemical Shift Index. A Fast and simple method for the assignment of protein secondary structure through NMR spectroscopy. *Biochemistry* **1992**, *31*, 1647–1651.
- (32) Titman, J.; Keeler, J. Measurement of homonuclear coupling constants from NMR correlation spectra. *J. Magn. Reson.* **1990**, *89*, 640–646.
- (33) Dyson, H. J.; Rance, M.; Houghten, R. A.; Wright, P. E.; Lerner, R. A. Folding of immunogenic peptide fragments of proteins in water solution. II. The nascent helix. *J. Mol. Biol.* **1988**, *201*, 201–217.
- (34) Guntert, P.; Mumenthaler, C.; Wüthrich, K. Torsion angle dynamics for NMR structure calculation with the new program DYANA. *J. Mol. Biol.* **1997**, *273*, 283–298.
- (35) Ding, X. Q.; Dolu, V.; Hadac, E. M.; Holicky, E. L.; Pinon, D. I.; Lybrand, T. P.; Miller, L. J. Refinement of the structure of the ligand-occupied cholecystokinin receptor using a photolabile amino-terminal probe. *J. Biol. Chem.* **2001**, *276*, 4236–4244.
- (36) Kennedy, K.; Gigoux, V.; Escrieut, C.; Maigret, B.; Martinez, J.; Moroder, L.; Frehel, D.; Gully, D.; Vaysse, N.; Fourmy, D. Identification of two amino acids of the human cholecystokinin-A receptor that interact with the N-terminal moiety of cholecystokinin. *J. Biol. Chem.* **1997**, *272*, 2920–2926.
- (37) Gigoux, V.; Maigret, B.; Escrieut, C.; Silvente-Poirot, S.; Bouisson, M.; Fehrentz, J.-A.; Moroder, L.; Gully, D.; Martinez, J.; Vaysse, N.; Fourmy, D. Arginine 197 of the cholecystokinin-A receptor binding site interacts with the sulfate of the peptide agonist cholecystokinin. *Protein Sci.* **1999**, *8*, 2347–2354.
- (38) Gigoux, V.; Escrieut, C.; Fehrentz, J.-A.; Poirot, S.; Maigret, B.; Moroder, L.; Gully, D.; Martinez, J.; Vaysse, N.; Fourmy, D. Arginine 336 and asparagine 333 of the human cholecystokinin-A receptor binding site interact with the penultimate aspartic acid and the C-terminal amide of cholecystokinin. *J. Biol. Chem.* **1999**, *274*, 20457–20464.
- (39) Silvente-Poirot, S.; Escrieut, C.; Galès, C.; Fehrentz, J.-A.; Escherich, A.; Wank, S. A.; Martinez, J.; Moroder, L.; Maigret, B.; Bouisson, M.; Vaysse, N.; Fourmy, D. Evidence for a direct interaction between the penultimate aspartic acid of cholecystokinin and histidine 207, located in the second extracellular loop of the cholecystokinin B receptor. *J. Biol. Chem.* **1999**, *274*, 23191–23197.
- (40) Dong, M.; Ding, X.-Q.; Pinon, D. I.; Hadac, E. M.; Oda, R. P.; Landers, J. P.; Miller, L. J. Structurally related peptide agonist, partial agonist, and antagonist occupy a similar binding pocket within the cholecystokinin receptor. Rapid analysis using fluorescent photoaffinity labeling probes and capillary electrophoresis. *J. Biol. Chem.* **1999**, *274*, 4778–4785.
- (41) Hadac, E. M.; Pinon, D. I.; Ji, Z.; Holicky, E. L.; Henne, R. M.; Lybrand, T. P.; Miller, L. J. Direct identification of a second distinct site of contact between cholecystokinin and its receptor. *J. Biol. Chem.* **1998**, *273*, 12988–12993.
- (42) Ji, Z.; Hadac, E. M.; Henne, R. M.; Patel, S. A.; Lybrand, T. P.; Miller, L. J. Direct identification of a distinct site of interaction between the carboxyl-terminal residue of cholecystokinin and the type A cholecystokinin receptor using photoaffinity labeling. *J. Biol. Chem.* **1997**, *272*, 24393–24401.
- (43) Anders, J.; Bluggel, M.; Meyer, H. E.; Kuhne, R.; ter Laak, A. M.; Kojro, E.; Fahrenholz, F. Direct identification of the agonist binding site in the human brain cholecystokinin B receptor. *Biochemistry* **1999**, *38*, 6043–6055.
- (44) Escherich, A.; Lutz, J.; Escrieut, C.; Fourmy, D.; van Neuren, A. S.; Müller, G.; Schafferhans, A.; Klebe, G.; Moroder, L. Peptide/Benzodiazepine-Hybrids as Ligands of CCK_A and CCK_B Receptors. *Biopolymers*, in press
- (45) Makovec, F.; Bani, M.; Cereda, R.; Chiste, R.; Pacini, M. A.; Revel, L.; Rovati, L. C. Antispasmodic activity on the gallbladder of the mouse of CR 1409 (lorglumide) a potent antagonist of peripheral CCK. *Pharmacol. Res. Commun.* **1987**, *19*, 41–51.
- (46) Chang, R. S.; Lotti, V. J. A potent nonpeptide cholecystokinin antagonist selective for peripheral tissues isolated from *Aspergillus alliaceus*. *Science* **1985**, *230*, 177–179.
- (47) Evans, B. E.; Bock, M. J.; Rittle, K. E. Design of potent, orally effective, nonpeptidic antagonists of the peptide hormone cholecystokinin. *Proc. Natl. Acad. Sci. U.S.A.* **1986**, *83*, 4918–4922.
- (48) Papini, A.; Rudolph, S.; Siglmüller, G.; Musiol, H.-J.; Göhring, W.; Moroder, L. Alkylation of histidine with maleimido-compounds. *Int. J. Pept. Protein Res.* **1992**, *39*, 348–355.
- (49) Marion, D.; Wüthrich, K. Application of phase sensitive two-dimensional correlated spectroscopy (COSY) for measurements of 1H–1H spin–spin coupling constants in proteins. *Biochem. Biophys. Res. Commun.* **1983**, *113*, 967–974.

JM0109457